

Near-field surface photovoltage

R. Shikler^{a)} and Y. Rosenwaks^{b)}

Department of Physical Electronics, Faculty of Engineering, Tel-Aviv University, Ramat-Aviv 69978, Israel

(Received 23 May 2000; accepted for publication 13 June 2000)

A phenomenon called near-field surface photovoltage is presented. It is based on inducing photovoltage only at a semiconductor space-charge region using near-field illumination. The photovoltage is obtained by measuring the contact potential difference between an optical near-field force sensor and a semiconductor surface under illumination. It is shown that the near-field illumination induces photovoltage at the surface which is principally different from photovoltage induced by far-field illumination. The mechanisms that govern the different far-field and near-field photovoltage response are discussed. © 2000 American Institute of Physics.
[S0003-6951(00)04132-2]

Surface photovoltage (SPV) is a well-established technique for the characterization of semiconductors, which is based on analyzing illumination-induced changes in the semiconductor surface potential, in a contactless, nondestructive manner. The method is based on the following principle. Illumination of a semiconductor surface by monochromatic light results in charge exchange between the bands, and between the band edges and local electron states, if the latter are present within the semiconductor band gap. The photogenerated charge may be transferred from the surface to the bulk (or vice versa) and/or redistributed within the surface or the bulk. As a result, the potential drop across the surface space-charge region (SCR), and hence, the surface potential changes. These changes are monitored by measuring the contact potential difference (CPD) under illumination between the semiconductor surface and a reference electrode.

The SPV method was first introduced by Brattain and Bardeen¹⁻³ and had found many diverse application over the years. For almost five decades, it has been used as an extensive source of surface and bulk information on various semiconductors and semiconductor interfaces.⁴ These research efforts have shed light on many scientifically and technologically important questions, especially in the areas of metal-semiconductor interfaces, semiconductor-insulator states, surface states passivation, bulk defects, and minority-carrier lifetime and diffusion length. To date, almost all the SPV-related techniques (apart from several preliminary reports mentioned below) have a common significant draw back: *they do not have high spatial and depth resolution.*

Scanning probe microscopy has opened opportunities to image electronic properties with unprecedented spatial resolution. Both scanning tunneling microscopy (STM),⁵ and atomic-force microscopy,⁶ have been modified to obtain high-resolution maps of the electric surface potential distribution. The applications of the STM are limited to conductive samples and are prone to influence from the measuring tip: In both the simple and synchronized-null STM schemes an electric field exists between the sample and tip due to the CPD between them, or due to an applied bias.⁴ This field

changes the surface potential of the sample and many measured features may stem from spatially resolved tip-induced bandbending.⁷

With the development of the Kelvin probe force microscopy (KPFM),⁶ this major disadvantage was overcome; this is because in the KPFM measurements the CPD between the sample and tip is nullified. The KPFM has found many diverse applications in recent years. It has been used to measure surface electronic properties like: charges,⁸ potential,⁹ photovoltage,¹⁰ and recently, minority-carrier diffusion length.^{11,12} KPFM has also proved to be effective in electrical characterization of submicron devices like high electron mobility transistors,¹³ and light-emitting diodes.¹⁴

By combining the KPFM with illumination, a high-resolution two-dimensional map of the SPV can be obtained. Higher spatial resolution SPV can be obtained by exciting a semiconductor using a nanometer-size light spot at exactly the same location where the CPD is measured by the KPFM tip. This can be achieved by using a sharp fiber tip like that used in the near-field scanning optical microscope, which also serves as the KPFM probe. In such a case, the semiconductor is excited with a laser passing through the near-field optical fiber which raster scans above the sample surface. Because the diameter of the fiber at the end of the probe is on the order of ≈ 50 nm ($\ll \lambda$, the illumination wavelength), the resulting illumination has a near-field profile.

In this letter, we show that such near-field illumination induces surface photovoltage which is principally different from photovoltage induced by far-field illumination. This near-field phenomenon, which we hereafter call the near-field surface photovoltage (NFSPV), introduces an additional depth dimension into SPV and KPFM measurements and paves the way for a variety of ultra-surface-sensitive SPV measurements and applications. The lateral resolution of the NFSPV technique is high because when the sample is in the near-field region of the tip (roughly within one aperture diameter from the end of the tip), the illumination spot size is determined by the diameter of the aperture at the end of the tip and is not limited by diffraction. The exact shape of the illumination area depends also on the permittivity and topography of the sample surface and on the exact tip shape and

^{a)}Electronic mail: shikler@post.tau.ac.il

^{b)}Electronic mail: yossir@eng.tau.ac.il

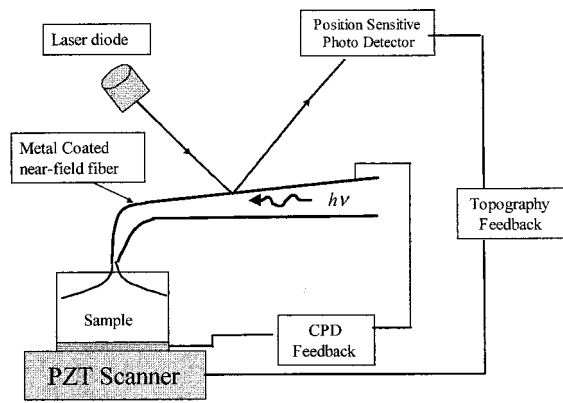


FIG. 1. Schematic diagram of the near-field surface photovoltage measurement system.

coating material; the SPV lateral resolution is governed by the minority-carrier diffusion length.

Figure 1 shows a schematic of the NFSPV measurement setup using an L-shaped optical fiber force sensor (Nanonics Supertips Inc.). It is fabricated from a single-mode optical fiber with special techniques for tapering such glass structures.¹⁵⁻¹⁷ The optical fiber tips were coated with gold, which served also as the electrical contact to the fiber through the fiber holder in the same way as for conventional tips. The fiber was vibrated by a piezo mounted above the cantilever. The KPFM measurements were carried out using a standard KPFM setup using Digital Instruments (Extended MultiMode Nanoscope III with the Extender Electronics Module) atomic-force microscope. All the measurements were conducted in air at ambient pressure and humidity; the measured sample was a GaP structure (Elma Inc.) consisting of $\approx 30 \mu\text{m}$ *p*-type layer grown on an *n*-type substrate.

The surface sensitivity of the NFSPV is demonstrated in the following way. The SPV, defined here as $\text{SPV} = \text{CPD}_{\text{light}} - \text{CPD}_{\text{dark}}$, of the GaP structure was measured using an argon-ion laser ($\lambda = 488 \text{ nm}$) under far-field and near-field illumination. Figure 2 shows the measured surface photovoltage as a function of the ratio between the light intensity (I) and the maximum light intensity ($I_0 \sim 12$ and $\sim 0.3 \text{ W/cm}^2$ for the near- and far-field illuminations, respectively) under near-field (top, solid line) and far-field illumination (bottom, dashed line). The dependence of the SPV on the illumination intensity is logarithmic as expected for super-band-gap illumination.¹⁸ Two main differences are observed in the results of Fig. 2. The first is that the sign of the SPV signal is opposite for the two illumination regimes: negative for the far-field, and positive for near-field illumination. The second difference is the slope of the SPV vs $\log(I)$ between the two cases. Super-band-gap SPV under low-injection-level conditions can be described by $|\text{SPV}| = (\eta kT/q) \ln(BI)$, where η and B are proportionality factors.¹⁹ Similar expressions for SPV have been obtained by different theoretical approaches like the depletion approximation,²⁰ the Schottky-diode model,²¹ and the constant quasi-Fermi-level approximation.²²

The different sign of the SPV in the two illumination regimes can be explained with the help of the band diagram of the GaP structure, presented in Fig. 3. The GaP band

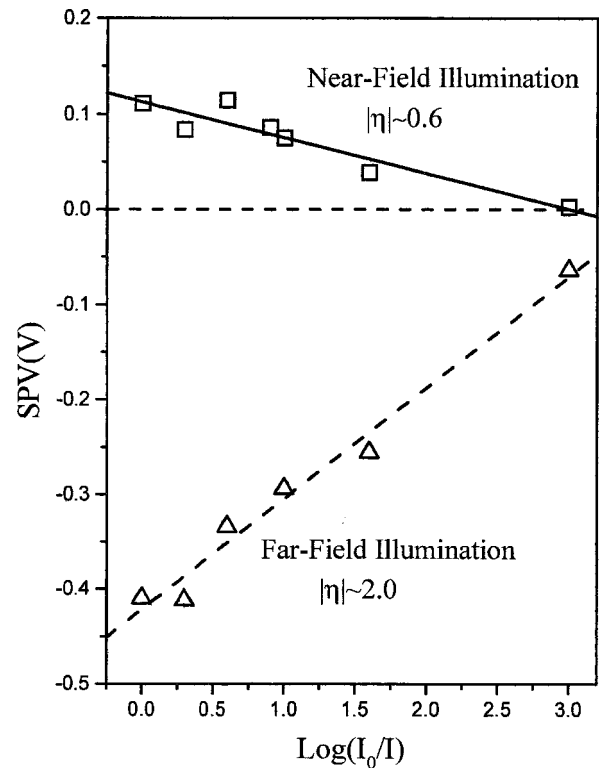


FIG. 2. Near-field (top) and far-field (bottom) surface photovoltage of a GaP structure as a function of the normalized illumination intensity.

structure includes two space-charge regions, one at the surface (the *p*-GaP surface depletion region) and the second is the buried *pn* junction. Under far-field illumination [Fig. 3(a), the dashed line] the light is absorbed in the two SCRs (the absorption length in GaP for $\lambda = 488 \text{ nm}$ is around $10 \mu\text{m}$). This results in a decrease of the built-in voltage in both

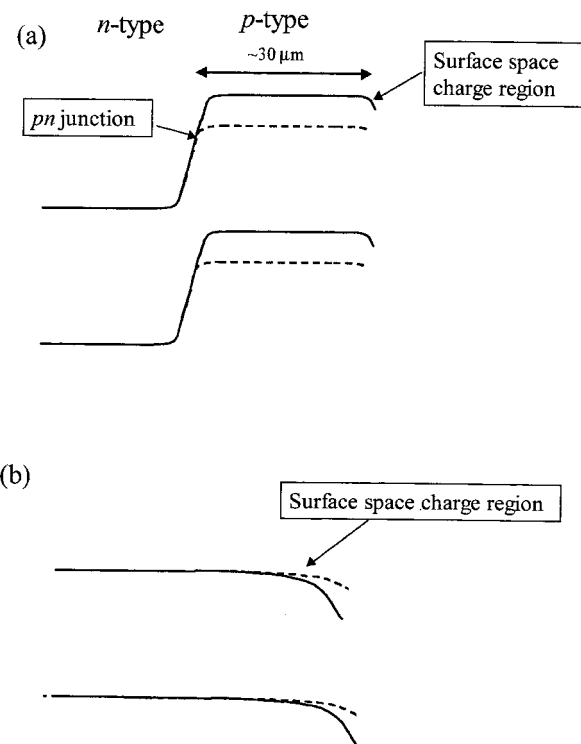


FIG. 3. Schematic band diagram of the GaP structure in the dark (solid lines), and under far-field (a) and near-field (b) illumination.

junctions due to the photovoltaic effect. Since the substrate is grounded, and due to the fact that the band flattening in the pn junction is much larger than the one in the surface SCR (due to larger built-in voltage), the SPV is governed by the buried junction, and thus it is negative as observed in the measurements (Fig. 2 bottom line).

The SPV response under near-field illumination is schematically described in Fig. 3(b), which shows only the p -GaP surface depletion region in equilibrium (solid line), and under near-field evanescent-wave excitation. The buried pn junction is not shown because the photocarriers are generated only in the vicinity of the surface SCR in the case of near-field illumination (the typical decay length for the near-field illumination is the aperture size, i.e., ≈ 50 nm). The excess carriers do not reach the buried pn junction by diffusion because the electron diffusion length in GaP is ≈ 2 μm ,^{11,12} and the thickness of the top p layer is 30 μm . Hence, the measured SPV is only due to band flattening of the surface SCR. For a depleted surface, the minority carriers (in this case, electrons) are swept toward the surface, thus reducing the bandbending there; this results in a positive SPV. Moreover, the SPV decreases with the decrease of the light intensity [increase in (I_0/I)]. This shows that the positive SPV obtained under near-field excitation is not due to lower light intensity. In summary, the NFSPV probes only the surface depletion region and not the buried pn junction.

The explanation for the different values of η obtained for the far- and near-field illuminations is more subtle. The magnitude of η quantifies the photovoltaic efficiency due to the photogenerated carriers. Under far-field illumination $\eta \approx 2$ because the photovoltaic process is due to the generation and recombination of both electrons and holes in the vicinity of the pn junction.²³ The excess carriers are then separated by the junction electric field and the electrons (holes) reduce the bandbending in the n side (p side) of the junction.

The absolute value of η at the surface cannot exceed 1 (Ref. 22) because only one type of carrier can reduce the bandbending. The surface bandbending is decreased either by positively charged surface states that capture an electron, or by screening when the illumination intensity is very large. The first process occurs when the cross section for electron capture by the surface states, σ_n , is much larger than the capture cross section for holes, σ_p , i.e., when $\sigma_n \gg \sigma_p$ (screening takes place when $\sigma_p \gg \sigma_n$ for a p -type depleted surface). A value of η that is smaller than 1 indicates that either the surface states cross sections for electrons and holes capture are of the same order of magnitude [$\sigma_n \approx \sigma_p$ (Ref. 22)], or that there is a large recombination rate in the space-charge region.¹⁹ When the two cross sections (σ_n and σ_p) are of the same order of magnitude, and once an electron is captured by a surface state, there is a large probability for a hole capture by the same state. This process reduces the band-flattening efficiency by the excess carriers and the value of η . The efficiency is also reduced when there is recombination in the space-charge region, because less carriers contribute to the photovoltaic effect.

The different values of η (≈ 0.6 for the near-field illumination and 2 for the far-field illumination) support our hypothesis regarding the surface sensitivity of the NFSPV. In

addition, these results are in agreement with the prediction of Bednyĭ and Baĭdus,¹⁹ who interpreted η as being equivalent to the ideality factor in a Schottky diode. Accordingly, η is ideal (i.e., 1) for a recombinationless barrier, and smaller than 1 when surface trapping of excess carriers is present.

In conclusion, we have presented a phenomenon called near-field surface photovoltage, based on band flattening due to near-field illumination. This method may find important applications both in semiconductor basic research and in technological applications. For example, it can be used to study SPV phenomena without the interference of bulk processes in semiconductors with very short diffusion length (GaN, for example). In addition, complex devices like thin-film transistors, high-electron-mobility transistors, and solar cells can be measured using the NFSPV with a reduced effect of the underlying layers. All these SPV measurements will also have high lateral resolution determined mainly by the minority-carrier diffusion length.

This research is supported by the Israel Science foundation administered by the Israel Academy of Science and Humanities—Recanati and IDB group foundation, and by Grant No. 9701 of the Israel Ministry of Science. One of the authors (R.S.) is supported by an Eshkol special scholarship of the Israel Ministry of Science.

¹W. H. Brattain, Phys. Rev. **72**, 345 (1947).

²W. H. Barattain and J. Bardeen, Bell Syst. Tech. J. **32**, 1 (1953).

³C. G. B. Garret and W. H. Brattain, Phys. Rev. **99**, 376 (1955).

⁴For a comprehensive review of surface photovoltage phenomena, see L. Kronik and Y. Shapira, Surf. Sci. Rep. **37**, 1 (1999).

⁵J. R. Kirtly, S. Washburn, and M. J. Brady, Phys. Rev. Lett. **60**, 1546 (1988); Y. Kuk, R. S. Becker, P. J. Silverman, and G. P. Lochanski, J. Vac. Sci. Technol. B **9**, 545 (1991).

⁶M. Nonnenmacher, O. Wolter, J. Greschner, and R. Kassing, J. Vac. Sci. Technol. B **9**, 1358 (1991).

⁷M. McElistern, G. Hasse, D. Chen, and R. J. Hamers, Phys. Rev. Lett. **70**, 2471 (1993).

⁸D. W. Abraham and H. K. Wickramasingh, Appl. Phys. Lett. **52**, 1103 (1988).

⁹C. Schonenberger and S. F. Alvarado, Phys. Rev. Lett. **65**, 3162 (1990).

¹⁰J. M. R. Weaver and D. W. Abraham, J. Vac. Sci. Technol. B **9**, 1559 (1991).

¹¹T. Meoded, R. Shikler, N. Fried, and Y. Rosenwaks, Appl. Phys. Lett. **75**, 2435 (1999).

¹²R. Shikler, T. Meoded, N. Fried, and Y. Rosenwaks, Phys. Rev. B **61**, 11041 (2000).

¹³T. Mizutani, M. Arakawa, and S. Kisimoto, IEEE Electron Device Lett. **18**, 423 (1997).

¹⁴R. Shikler, T. Meoded, N. Fried, and Y. Rosenwaks, Appl. Phys. Lett. **74**, 2972 (1999).

¹⁵A. Harootunian, E. Betzig, M. Isaacson, and A. Lewis, Appl. Phys. Lett. **49**, 674 (1982).

¹⁶S. Shalom, K. Lieberman, A. Lewis, and S. R. Cohen, Rev. Sci. Instrum. **63**, 4061 (1992).

¹⁷K. Lieberman, A. Lewis, G. Fish, S. Shalom, T. M. Jovin, A. Schaper, and S. R. Cohen, Appl. Phys. Lett. **65**, 648 (1994).

¹⁸L. Kronik, M. Leibovitch, E. Fefer, L. Burstein, and Y. Shapira, J. Electron. Mater. **24**, 379 (1995).

¹⁹B. I. Bednyĭ and N. V. Baĭdus, Semiconductors **27**, 431 (1993).

²⁰R. Williams, J. Phys. Chem. Solids **23**, 1057 (1962).

²¹L. K. Galbraith and T. E. Fischer, Surf. Sci. **30**, 185 (1972).

²²O. B. Apeh, L. Kronik, M. Leibovitch, and Y. Shapira, Surf. Sci. **409**, 485 (1998).

²³S. M. Sze, *Physics of Semiconductor Devices*, 2nd ed. (Wiley, New York, 1985).